Development of a Chewing Robot with Built-in Humanoid Jaws to Simulate Mastication to Quantify Robotic Agents Release from Chewing Gums Compared to Human Participants

Kazem Alemzadeh*, Siân Bodfel Jones, Maria Davies and Nicola West

Abstract— **Medicated chewing gum has been recognised as a new advanced drug delivery method, with a promising future. Its potential has not yet been fully exploited because currently there is no gold standard for testing the release of agents from chewing gum *in vitro*. This study presents a novel humanoid chewing robot capable of closely replicating the human chewing motion in a closed environment, incorporating artificial saliva and allowing measurement of xylitol release from the gum. The release of xylitol from commercially available chewing gum was quantified following both *in vitro* and *in vivo* mastication. The chewing robot demonstrated a similar release rate of xylitol as human participants. The greatest release of xylitol occurred during the first 5 minutes of chewing and after 20 minutes of chewing only a low amount of xylitol remained in the gum bolus, irrespective of the chewing method used. Saliva and artificial saliva solutions respectively were collected after 5, 10, 15 and 20 minutes of continuous chewing and the amount of xylitol released from the chewing gum determined. Bioengineering has been implemented as the key engineering strategy to create an artificial oral environment that closely mimics that found in vivo. These results demonstrate the chewing robot with built-in humanoid jaws could provide opportunities for pharmaceutical companies to investigate and refine drug release from gum, with reduced patient exposure and reduced costs using this novel methodology.**

***Index Terms*—Chewing Robot, Mechanical Occlusion, Chewing Efficiency, Medicated Chewing Gum, *In Vitro - In Vivo* Drug Release Xylitol, Saliva.**

I. Introduction

CHEWING a gum type substance has been a habit since ancient times when resin from the sapodilla tree was chewed to clean teeth and freshen breath [1]. More recently confectionary chewing gum has been chewed for its sweetness and fresh taste [2]. Sugar free gum is also recommended by oral healthcare professionals for its caries preventative properties when consumed following mealtimes to recover the acid pH within the mouth [3]-[4]. Chewing gum has also been identified as a useful mode of drug delivery and is recognised under the term medicated chewing gum (MCG). The first example of a commercial MCG was launched in 1928 as Aspergum® which contained acetylasilic acid to alleviate headaches and is still commercially available in the USA [5]. Since then other drugs have been added to chewing gum with the most recognised product being Nicotine, successfully launched in the 1980's as a substitute to smoking cigarettes and as an aid to smoke cessation [6]. Other examples of agents that have been included in MCG are aspirin, caffeine, dimenhydrinate, calcium carbonate, vitamin C, fluoride and chlorhexidine [5]. Recent studies suggest curcumin (CUR) chewing gums have potential therapeutic benefits to head and neck cancer patients [7]-[9].

There are several advantages to delivering pharmaceutical agents through chewing gum rather than conventional tablets that are usually swallowed with water. The greatest advantage being that the agent can be absorbed through the oral mucosa thus avoiding metabolism in the gastrointestinal tract and reducing first pass metabolism. A lower concentration of the agent can be prescribed because it has more bioavailability and a faster onset of action when it is absorbed into the blood circulation if delivered in this way [5], [10]. Other advantages include the fact that it is easy to administer for children and the elderly, does not require water for administration, can provide sustained drug release over time as well as being localised to target specific conditions in the oral cavity. Variation in the release rate of the agent which is determined by the chewing action and force of each individual, needs to be considered, as does the potential to swallow the gum.

There have been limitations in the development of MCG due to difficulties in simulating the human masticatory action *in vitro* whilst also passing fluid over the artificial gum surface to enable the release of the pharmaceutical agents from the gum,

Manuscrip received January 30, 2020.

K. Alemzadeh is with the Faculty of Engineering, Department of Mechanical Engineering, University of Bristol, Bristol, BS8 1TR. UK. (*k.alemzadeh@bristol.ac.uk) ORCID: http://orcid.org/0000-0002-9127-5530. Siân Bodfel Jones, Maria Davies and Nicola West (http://orcid.org/0000-0003-1522-961X) are with the Applied Clinical Trials Unit, Bristol Dental School, University of Bristol, Bristol, BS1 2LY. UK.

mimicking the human oral environment.

Review of the literature demonstrates mastication apparatus have been developed for three main applications. These are i) food science where the focus is bolus breakdown and flavour release [11]-[14], ii) dental science where the main focus is on material testing and failure points [15]-[17] and iii) the pharmaceutical industry for drug release [18]-[19].

Within food science the two most commonly used apparatus are the 'AM2 apparatus' which was developed by Alain Woda *et al.* [14] and the 'artificial mouth' developed by Christian Salles *et al.*[13]. The AM2 apparatus has been used to determine the breakdown of the food to form a bolus that can be easily swallowed [14] as well as highlighting variances between the type of bolus that is created depending on variances within mastication [20]. The apparatus design has most of the biomechanical masticatory features found in humans compared to other bolus forming mastication apparatus. The 'artificial mouth' designed by [13] has previously been used to determine the aromas that are created as the food bolus is formed for flavour determination [21]. It encompasses more of the physiological purposes than other apparatus that are used within food science. A review by Peyron and Woda [12] has highlighted five key principles to consider when designing a mastication simulator that is used for food science investigations. These are i) the incorporation of teeth or equivalent, ii) the volume inside the chamber, iii) the inclusion of saliva or equivalent solution, iv) maintaining temperature control and v) the kinetics and stress modalities of functioning. Although they have reviewed many simulators that claim to be adequate for various investigations, not many are found to incorporate these key five principles. A well-designed simulator should also be validated against human mastication *in vivo* and this is not commonly undertaken when designing new simulators.

Some instruments designed specifically for testing dental materials are open systems therefore it is not possible to hold chewing gum in place [22]-[23]. Previous work by Alemzadeh and Raabe [15] developed a chewing simulator that replicates the temporomandibular joint and allows the six degrees of freedom but again it is an open system so cannot be used to investigate MCG. In order to investigate the release of active pharmaceutical ingredient (API) from MCG, the instrument needs to be a closed system that allows solution to pass over the occlusal surfaces and to be collected in order to quantify the release of substances from chewing gums.

There are currently two chewing instruments recognised by the European Pharmacopoeia which are specifically designed for testing MCG *in vitro*, Apparatus A [18] and Apparatus B [19] developed by Christrup and Møller 1986 and Kvist et al., 1999 respectively. Apparatus A consists of a non-transparent metal chamber which holds the gum and solution. It has two horizontal oscillatory pistons to simulate the jaw and one vertical piston to keep the gum in place. It is recommended to use 20 ml of phosphate buffered saline at pH 6 as the solution surrounding the gum and for the chamber to be heated to 37ºC [10], [18], [24]-[25]. Apparatus B consists of a double walled glass chamber with one lower vertical piston which moves up and down and one upper vertical stationary but rotating piston. The solution is agitated during the chewing simulation. The distance between the chewing platforms, the frequency of the chewing strokes, the angle of the twisting during chewing and the temperature of the chamber can all be adjusted [19]. Changing these parameters has previously shown a variation in the degree of agents released from MCG [19], [26]. Ultimately the purpose of developing a chewing simulator is to have an instrument that will accurately simulate the human chewing action to reproducibly provide information that correlates with that obtained when using human participants. Apparatus B has been shown to successfully quantify the release of various agents from MCG. It provided results that were similar to using trained human participants to chew gum [26]. The instrument is primarily designed to compare batches of gums as a quality control instrument but can also be useful as a research and development tool [26], [27]. It has been presented as a simplified and standardized model of the human jaw but with potential limitations with respect to *in vivo* predictive capabilities. For example, the simplicity in the design of the instrument limits its capability to fully mimic the complex physiological conditions in the oral cavity during chewing [27]. Further limitations are outlined below.

Previous work comparing both apparatus A and B [25], [28]-[30] observed that the *in vitro* drug release from the chewing gum formulations varied significantly with respect to the apparatus and the products being used. When using apparatus A no discriminatory drug release profiles under different test conditions could be generated, whereas with apparatus B, release profiles was higher using apparatus B than A. This is due to the additional twisting motion induced by the apparatus during mastication [29].

More recent work in 2017 by Stomberg and co-workers [31] looking at the dissolution rates of soft chewable dosage forms highlighted "the principle of both methods A & B is a stamping procedure between two flat-faced, optionally rotating pistons. A further vertical piston in method A guarantees the right position of the gum between two horizontal ones. These methods describe chewing as a consistent process". Due to this mastication simplification, the authors suggested an adjustment to the apparatus, the samples being placed on a 45º gliding steel unit, shaped like a human molar tooth [31]. The gliding unit attempted to imitate the occlusal plane of the natural dentition with the simulator squeezing the gum by a pre-set deformation force [31]. However, despite the authors valiant attempts, the four cusped molar tooth apparatus had limited occlusal surface anatomical accuracy and the mastication was very simplified.

In 2019 Externbrink and co-workers [27] highlighted a need for new testing methodologies to evaluate the performance of potentially abuse-deterrent opioid products by chewing and reviewed both A & B apparatus and highlighted that Apparatus B has been described in the scientific literature and is commercially available (Erweka release tester, Erweka GmbH). They used Apparatus B and the results of their study indicates that the chewing methodology evaluated in their work may provide a useful *in vitro* tool to characterize the chewing resistance of a drug product and its drug release properties

following chewing. Overall, the chewing apparatus provides a simplified and standardized model of the human jaw with limited capability to fully mimic the complex physiological conditions in the oral cavity during chewing.

Humans have a masticatory system that includes the lower jaw (mandible) and the upper jaw (maxilla) which are connected at the temporomandibular joint. The temporomandibular joint and the surrounding muscles determine the movement of the mandible and unlike other joints in the human body allows six degrees of freedom.

A chewing simulator should ideally replicate the mechanics of dental occlusion or mechanics of mastication requiring the engineering of dental occlusion principles [32]-[36] and physiological features [37] associated with relationships between tooth form and chewing motions [38] to define three types of food processing; shearing, crushing and grinding [38]-[41], which neither Apparatus A or B fully take into consideration. For foodstuffs, including chewing gum, to be effectively processed through mastication, mechanics of chewing sequences, shearing, crushing and grinding of the bolus need to take place [38]-[42]. To maximise the crush/shear ratio for optimum chewing efficiency [40]-[42] the Bennet movement of the mandible [43], Andrews's six key occlusion principles [44] and occlusal curvatures [45] such as the Curve of Spee [46]-[47], Curve of Wilson [48] and Sphere of Monson [49] should be implemented. The MCG's potential has therefore not yet been fully exploited.

The aim of this study was to validate a novel closed system chewing robot for assessment of MCG. The robot is designed to more accurately replicate human mastication by incorporating the movements of the temporamandibular joint whilst also facilitating saliva to flow over the tooth occlusal surfaces. The amount of xylitol remaining in the bolus was assessed as the primary aim and compared between the chewing robot and human participants. As a secondary aim was to assess the amount of xylitol released from chewing the gum.

II. DEVELOPMENT OF THE HUMANIOD CHEWING ROBOT

A. Design and Modeling

A digital skull model was reverse engineered from an artificial human skull (SOMSO® MODELLE GmbH, Adam Rouilly Kent, UK) using RE Imageware® V13.0 and CAD/CAM/CAE NX Siemens® V11.0 software. The skull is composed of two parts: the cranium with the upper jaw (maxilla) and the lower jaw (mandible), both with their respective teeth. The process from digitisation, alignment, landmark identification and clinical registration to surface and solid modelling and final prototyping is illustrated in Table I. The model product design specification (PDS) strategy was based on bioengineering [50]-[53], biomimetic and biologically inspired design [54]-[59] as the key engineering driver/solution to maintain design and manufacturing anthropomorphic properties of the human skull. This was dictated by study of skull anatomy, bones, muscles, in particular dentition and occlusal surfaces to understand functional morphology of the bones and the mechanism of chewing to overcome the major limitation of apparatus A and B to engineer a mechanical chewing robot.

In phase 1 3D geometric morphometric analysis was carried out to identify the critical regions of the skull that must be aligned to optimise the digitising process, using a series of photographs from different angles to design different grids as shown in Table I a). Special fixtures were then designed to help digitisation process, aiding to identify clinical Landmark and registration processes. In phase 2 referential geometrical entities (RGEs) and 3D cephalometric analysis (CeA) were carried out to identify and construct the three anatomical planes (the sagittal plane, the Frankfurt plane & the coronal plane) for best alignment using 1) basion, nasion and sella point on maxilla and 2) the infradental, gnathion on the mandible as shown in Table I b,c. The image represents the skull with its clinically registered point cloud which was used for segmentation and feature extraction process using Imageware® software. In phase 3 features extraction and segmentations were carried out to identify facial bones (i.e. frontal, orbits, nasal, Zygomatic, temporal and cheek) and teeth as shown in Table I d,e) respectively. Table I e) shows mandibular teeth morphological traits, such as cusp boundary curves, occlusal surfaces for lingual and buccal sides. Teeth have different numbers of cusps, the greatest number being seen on the molar teeth and Table I f,g show details of the 3D feature extraction of a 3rd molar with the cusps on the crown. Table I f) shows the detail of 3D feature extraction of a 3rd molar optimum tooth/cusps morphology and Table I g) shows surface quality analysis with needle plot, indicating values of the error which is the difference between the cusps surfaces created and the corresponding point clouds - (the maximum and average values are 101 µm and 7.5 µm respectively). In phase 4 the chewing trajectory information [60] was digitised and combined with the origin and insertion coordinates (x, y, z) of muscle lines of action [61] which were mapped and constrained to the digital model before multi-body dynamic simulation. Table I h) shows the frontal view of the digital skull with chewing trajectory information such as left/right condylion (which defines geometric kinematic axis & incisor points). Table I i) shows sagittal view of the muscle data (7 on each side). Table I i, j) show the springs representing the temporalis muscle. Its direction was derived by finding the resultant of the anterior and posterior temporalis. The line representing the resultant was extended until it intersected with the mandible at a suitable location and an insertion attachment feature was created at this point. Similarly for the origin point attachment a feature was created where the line intersected with the maxilla. Table I i, shows also the sagittal view of the alternate bilateral chewing bionic design with the removable mandibular and maxillary teeth. In phase 5, dynamic analysis and optimisation of chewing forces with muscle data was carried out, Table I k) shows the digital humanoid skull model with chewing trajectory and mechanical muscle actuators, where muscle insertions and origins were selected on both the mandible and maxilla respectively. Table I l, shows isometric view of the alternate bilateral chewing bionic design with functional springs after

removal of unnecessary skull features. In phase 6 both robots were prototyped to prove the concept, Table I m) shows the fully functional humanoid prototype whilst n) shows isometric view of the 4-bar linkage alternate chewing robot with built-in humanoid jaws. It is worth mentioning that the artificial human skull used in this study had no tooth loss, with normal occlusion, no dysfunction of the temporomandibular joint and without craniofacial skeletal changes. This is not a representative of large populations, however the digital skull model can easily be modified to represent various dental scenarios.

TABLE I

Bioengineering Design Phases of the Humanoid Chewing Robot
The Reverse engineering processes from digitisation, alignment, landmark identification, clinical registration and features extraction to surface and solid modelling and final prototyping

- Phase 1 – The 3D geometric morphometric analysis (GMA)	**- Phase 2 -** The referential geometrical entities (RGEs) and the use of 3D cephalometric analysis (CeA)
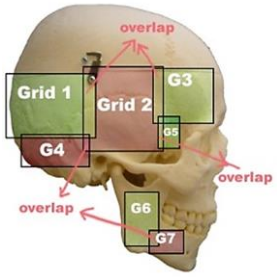 a)	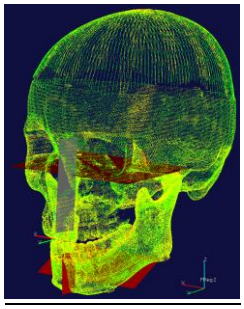 b) 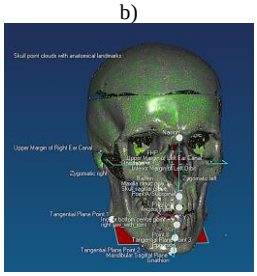 c)
- Phase 3 – RGEs features extraction and segmentations based on dental morphology and anatomical landmarks	**- Phase 4 -** Mapping chewing trajectory, clinical alignment, chewing motion with correct forces and identification number of bilateral functional springs attached to the maxilla.
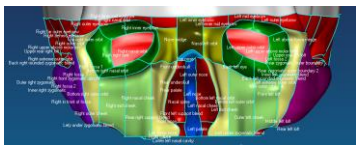 d)	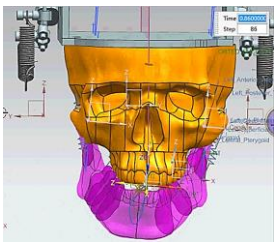 h)

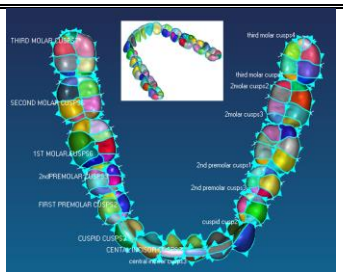 e) 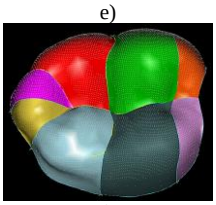 f) 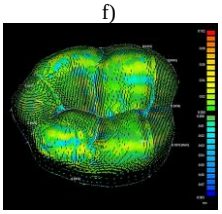 g)	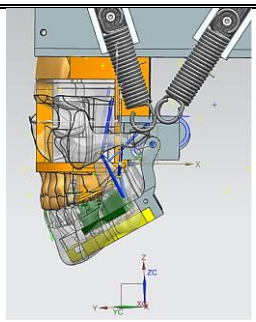 i) 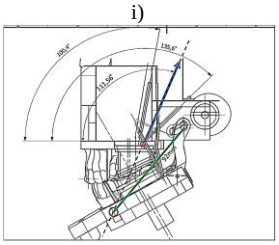 j)
- Phase 5 – Dynamic analysis and optimisation of chewing forces with muscle data	**- Phase 6 -** Fully functional prototype
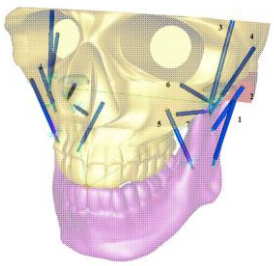 k)	 m)
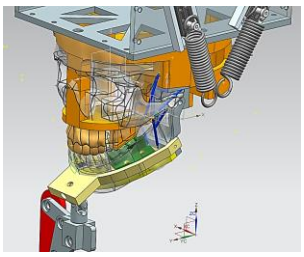 l)	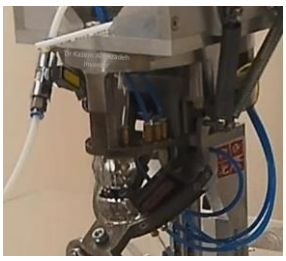 n)

B. *Methods and Processes*

Medical reverse engineering (MRE) technology and advanced computer-aided design and computer-aided manufacture (CAD/CAM) has been used in conjunction with PDS strategy to design and develop the artificial oral environment built-in to digital skull using digitisation, segmentation (features extraction), surface/solid modeling as described in section A [62]. Reverse engineering (RE) has been used as a strategy to maintain the accuracy and integrity of the processes between anatomical Landmarks and representation of biological structures in the 3D design space for a skull [63]-

[68]. It ensures that the reconstruction of the mandible, maxilla, mandibular condyle and temporomandibular joint (TMJ) meet the correct restoration of articulation, occlusion and mastication from a functional and correct shape point of view. The 3D geometric morphometric analysis (GMA) [69]-[75], the referential geometrical entities (RGEs) [63], [67]-[68], [71]-[72], [76]-[82] and the use of 3D cephalometric analysis (CeA) [83]-[87] have been integrated into the RE strategy. Analysis tools like 3D GMA and RGEs can determine biological shapes, anatomical landmarks and three anatomical planes respectively, with the 3D CeA able to relate the geometry of the planes of the mandible to the skull for characterising the dental and skeletal relationships for clinical registration and occlusion. The novel RGEs developed were based on dental morphology and anatomical landmarks to drive the bionic design strategy and processes for correct clinical alignment, segmentation and features extraction. The RGEs methods were also applied to extract accurate morphological traits in teeth and the condyles' centre of rotation. The reason that RE [64]-[66] was chosen as a strategy is because it has a powerful design tool for model modification needed for obtaining an optimal product design. In other words, the RE allows design methods, functional principles, engineering constraints and aesthetical evaluations to be represented by point cloud positions and their differential geometric attributes into shape reconstruction processes normally involves digitisation, segmentation, surface and solid modeling respectively as presented in Table I.

C. Multi-body Dynamics Analysis

The bionic digital skull was then further used to investigate and test the kinematic structure in conjunction with multi-body dynamics simulation based on rigid body spring model (RBSM) [88] to visualise the performance of the digital skull for being anatomically correct. Clinical chewing trajectories (sagittal & frontal) [60] were mapped into centre of condyles and incisor tip with the muscle data [61] respectively to aid this as highlighted in Table I, k and enlarged in Fig. 1.

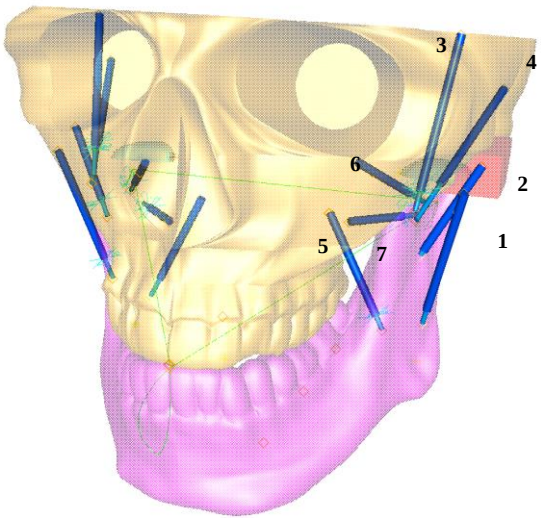

Fig. 1 An enlarged version of Table I, k showing the digital skull model with chewing trajectory and mechanical muscle actuators, where muscle insertions and origins were selected on the mandible and maxilla respectively. 1, superficial masseter; 2, deep masseter; 3, anterior temporalis; 4, posterior temporalis; 5, anterior medial pterygoid; 6, posterior medial pterygoid; 7, inferior lateral pterygoid.

These were used to simulate the bionic mandible and forces necessary during chewing, as these mechanical actuators can extend and contract during the chewing cycle while the incisors followed tear-drop shape chewing trajectory with 1 chew/second [60]. Accurate identification of the Bonwill triangle (green colour) on the mandible is the key to the successful bionic mechanism design. This triangle defines the characteristics of the mandible. Fig. 1 shows the biological rigid bodies and how they were defined as a mechanical system. The mandible has been constrained to the maxilla with the temporomandibular joint (TMJ) disc between them to move in six degrees of freedom similar to the human jaw. NX Siemens® software was used to analyse the developed bionic model kinematically and dynamically. The interaction between rigid bodies, contacts between two surfaces, positioning of the contacts and material properties of the skull structures all had to be carefully modelled, ensuring that the softer materials like the TMJ disc (cartilaginous disc that separates the condyle and temporal) deformed under pressure and that the compression and expansion of the disc moved the condyle accurately before the removal of unnecessary skull features for prototyping of the final chewing robot was done.

Once this was achieved, the mechanical actuators were replaced with a 4-bar linkage chewing mechanism for the new bionic design. Further dynamic analysis showed that the mechanism attached to the mandibular chin consists of a chain and cam which are synchronised, allowing the robot to chew at 60 chews per minute [19], [24], [28-30] when the mechanism handle is turned as shown in Table I, l. The use of 4-bar linkage to describe 2D planar chewing trajectory was reported by Weiliang Xu *et al.* [89] and they developed a chewing device with six-bar crank-slider linkage for food evaluation [89] and [90]. In 2016 Singhatanadgit and co-workers [91] adapted the 4-bar linkage mechanism for a new masticatory simulator to create loading patterns to test mechanical responses of the dental material test specimen.

Multi-body dynamic simulation also identified that two bilateral functional springs attached to each side of the maxilla of the digital skull were sufficient for holding the mandible in the correct mechanical occlusion and balance the torque generated during chewing whilst being in contact with the mandible condyles and cam system. Attached to the mandible condyles is an axle connected to the left and right condyle brackets with bilateral functional springs attached to the maxilla of the replica skull. These springs allow various forces to be applied to the bolus and therefore the force applied to the bolus changes in accordance to its stiffness. The condyle brackets with built in chewing pattern and bilateral springs aim replicate the Bennet movement of the mandible. The attached chewing mechanism allows the robot mandible to move in the sagittal plane and allows occlusal curvatures such as curve of Spee, curve of Wilson and sphere of Monson to be replicated as shown in Table I, i,l. Finally, a mechanically driven chewing

robot was prototyped to verify natural movements to optimise mechanical occlusion, mechanics of chewing, chewing motion and chewing forces necessary for testing MCG *in vitro*.

D. Prototyping the Humanoid Chewing Robot

The humanoid chewing robot consists of three main parts; Fig. 2, a) the custom-built simulator with humanoid jaws, b) a custom-built control box and c) a water bath (Cole-Parmer Instrument Company Ltd, Cambridgshire, UK).

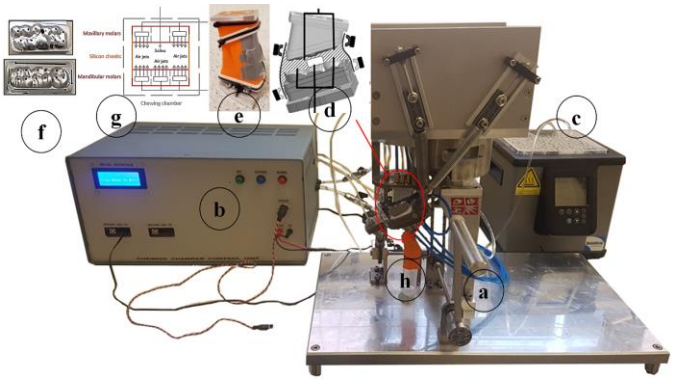

Fig. 2 a) the custom-built simulator with humanoid jaws, showing sagittal view of 4-bar linkage mechanism drive attached to the mandibular chin and occluded to maxillary jaw. b) the custom-built control box contains pumps, pneumatic solenoid valves and microcontrollers to simulate the oral environment. c) a water calibrated bath for heating the chewing chamber to maintain its temperature at the body level (37°C) using a diaphragm micro pump which circulates heated water through internal tracks designed in the mandible and maxilla. d) the removable chewing chamber contains a set of maxillary and mandibular replica teeth with the chewing gum in position e) silicon artificial cheeks that are used to encapsulate the chewing chamber preventing the gum from leaving and the artificial saliva from leaking f) surface of the teeth in the chewing chamber showing holes where air and artificial saliva enter and g) schematic showing the flow of air and artificial saliva into the chewing chamber to allow the gum to move as it would in a human mouth. h) contaminated saliva collection tube for later analyses.

The simulator has three main parts; a modified replica of a human skull, a removable chewing chamber and the chewing mechanism which attaches to the anterior region of the replica mandible. Fig. 2, a) skull shows unnecessary facial features were removed from the maxillary jaw to aid delivery of the air jets and artificial saliva and additional attachments were fabricated for the bilateral springs which attached to each side of the skull to hold the mandible in the correct mechanical occlusion.

The removable chewing chamber (Fig. 2, d-f) contains a set of maxillary and mandibular replica teeth and it is encapsulated by silicon artificial cheeks which prevent the gum from leaving the chamber and avoid artificial saliva leakage. Holes in the teeth allow pressurised air and artificial saliva to be delivered into the chamber which is controlled by two electronic pneumatic valves used in built-in control box with their own controller. Pneumatic manipulation of the chewing gum simulates the action of the cheeks and tongue to re-shape and re-orient the chewing gum when mandible jaw is fully opened. While artificial saliva is delivered into the chewing chamber when the mandible jaw is fully closed. The synchronisation of the air jets operation and artificial saliva delivery have been optimised with extensive testing.

Fig. 2, a) the simulator shows the mechanism handle attached to the shaft connected to the 4-bar linkage, attached to the mandibular chin. When the handle is turned it produces a constant rotational torque of 5 Nm at the joint, which in turn is transmitted to a crank creating the chewing motion. The chewing cycle has a duration of 1 second, opening and closing allowing 60 chews per minute [19], [24], [28-30], conforming with the chewing frequency used for the two chewing simulators recognised by the European Pharmacopoeia [24]. The chewing mechanism allows the maximum displacement between the maxillary and mandibular teeth in the chewing chamber to be 6.5 mm.

The temperature of the chewing chamber was regulated at 37°C with a temperature calibration water bath integrated with the control box. The water was supplied through internal tracks in the mandible and maxilla with a diaphragm micro pump circulation system (KNF Neuberger Ltd, Oxfordshire, UK). Fresh artificial saliva was used for each gum chewed. The control box also simulated the increasing and decreasing production of artificial saliva delivered into the chewing chamber over the 20 minute chewing period [92]. A tube was attached external to the chewing chamber via a connecting tube to collect the artificial saliva containing the released agents from the gum. A new collection pot was used every 5 minutes over the 20 minute chewing cycle thus providing a new sample for analysis after each 5 minutes of chewing.

E. Artificial Saliva Flow Rate

The amount of artificial saliva that was pumped into the chewing chamber was either 23.5 ml (samples 3, 4 and 5) or 47 ml for all other samples over the 20 minute chewing period. This amount was calculated based on clinical data received from the work of Cecilia Dong *et al.* [92] and our own in-house calculations based on the amount of artificial saliva that would evaporate due to the air jets manipulation of the chewing gum. Artificial saliva was continuously added to the chewing chamber over the 20 minute chewing period. The highest amount of saliva was delivered over the first five minutes with a maximum rate of 4.9 ml/min decreasing to 1.2 ml/min by the final five minutes when 23.5 ml artificial saliva was used. These amounts were doubled when the increased amount of 47 ml was used. Artificial saliva contained 0.7mM calcium chloride dihydrate, 0.2mM magnesium chloride, 4mM potassium dihydrogen phosphate, 20mM HEPES, 30mM potassium chloride and 0.1mM hydrochloric acid, pH adjusted to 6.8 using potassium hydroxide.

F. Preparing Samples and Chewing

Prior to commencement of robotic chewing, each chewing gum was weighed and the weight recorded using a microbalance (ATP Instrumentation Ltd, Leicestershire, UK). Ten replicas of the chewing chamber consisting of maxillary & mandibular teeth surrounded with artificial cheeks, which encapsulated the chewing gum, were prepared in a clean

environment prior to testing. These chambers were used to investigate the test chewing gum, Wrigley's Extra White® (The Wrigley Company, Plymouth, UK), containing xylitol as the investigative agent. A further 10 chewing chambers were also prepared containing Hubba Bubba Seriously Strawberry gum® (The Wrigley Company, Plymouth, UK) as a negative control with no xylitol present in the gum (data not presented here). Each chewing chamber was loaded one at a time into the simulator. Artificial saliva passed through the system whilst an operator manually turned the handle of the chewing simulator maintaining a constant speed of 60 chews per minute [19], [24], [28-30]. The simulator was operated for a continuous period of 20 minutes. The solution was collected from a tube connected to a collection vessel external to the chewing chamber at 5 minute intervals (following 5, 10, 15 and 20 minutes of chewing). The chewing simulator was flushed with deionised water and artificial saliva between each 20 minute cycle and prior to inserting the next chewing chamber to avoid any carry over. After each 20 minute cycle the collected artificial saliva was frozen until analysis. Every part of the chewing gum bolus was recovered from within the chewing chamber and weighed prior to dissolving for analysis.

G. *Chewing Using Human Participants*

Ethical approval was provided from the University of Bristol Faculty of Health Sciences Research Ethics Committee (application # 30882) so that 10 healthy adult dentate subjects who provided written informed consent were recruited to chew gum and expectorate into a sterile vessel. This number of participants is in line with the number used in other similar studies [19], [24], [28-30]. Exclusion criteria for participating in this study consisted of the use of daily medication that may cause dry mouth, wearing of orthodontic appliances and any known intolerance or hypersensitivity to the chewing gum. Participants refrained from eating any known xylitol containing food for 24 hours prior to taking part and were trained to chew and expectorate their saliva. Each subject chewed the Wrigley's Extra White chewing gum for 20 minutes and expectorated their saliva into a sterile vessel when required. A new vessel was used for collection of saliva every 5 minutes so that the amount of saliva collected represented the total amount of saliva expectorated after 5, 10, 15 and 20 minutes of chewing. The weight of each gum pre and post chewing was recorded.

H. *Determining the Amount of Xylitol in Saliva Solutions and gum bolus*

Following chewing by either the robot or the human participants, the bolus and saliva solutions were analysed to determine the amount of xylitol present. Alongside this the original amount of xylitol available in the gum was measured from 10 unused pieces of chewing gum. The total amount of xylitol determined in the solution and gum bolus was compared to the known total amount of xylitol available in an unused piece of gum.

The volume of saliva collected from each participant after 5, 10, 15 and 20 minutes of chewing was recorded. A sorbitol/xylitol enzymatic kit (Megazyme, Megazyme International Ireland Limited, Wicklow, Ireland), and a UV-Vis spectrophotometer (Aquarius, Cecil Instruments, Cambridge, England) set at a wavelength of 492 nm were used to quantify the amount of xylitol in solution. The enzymatic kit instructions were followed for xylitol analysis.

Standard solutions of xylitol were prepared in artificial saliva (0.05, 0.10 0.15 and 0.20 µg/ml) and a standard curve obtained. The amount of xylitol in solution was calculated from the standard curve.

I. *Dissolving Chewing Gum Bolus and Fresh Chewing Gum*

The amounts of xylitol present in an unused piece of chewing gum and in the bolus after 20 minutes of chewing were analysed following dissolution. The chewing gum/bolus was weighed and dissolved in a mixture of 3 ml toluene and 6 ml deionised water using a multi rotator (PTR-60 Grant-bio, Grant Instruments Ltd, Cambridgeshire, UK) until the gum dissolved. The solution was centrifuged (Denley BS400, Yorkshire, UK) at 1500 g in sealed polypropylene tubes for 10 minutes.

The upper layer of toluene was removed and discarded leaving the dissolved xylitol in the remaining 6 ml aqueous phase. These solutions were then diluted as necessary using deionized water so that their concentrations were between the upper and lower bounds of the concentrations of the standard curve solutions as outlined in (H). The amount of xylitol could then be quantified using the enzymatic kit and a linear calibration curve.

J. *Statistical Analysis*

A Mann Whitney statistical test was used to compare the amount of xylitol that was collected following each time period from both chewing mechanisms. The IBM SPSS statistics 24 software package was used for all analyses.

III. RESULTS

A. *Chewing Force Experiments*

Force measurement experiments were carried out to set correctly the bilateral springs to allow initial breakdown of the gum. Fig. 3 shows the results of measuring the initial force required to break the shell of the chewing gum using an Instron 50KN 2580 series Static Load Cell (Instron, Massachusetts, USA). The results from the Instron Static Load Cell showed that an initial force of between 200 and 250 N was required to break the hard shell of the chewing gum. However, this force does not fully represent the force that would be required within the chewing chamber because the occlusal surface of the chewing chamber is more defined than the flat platform of the static load cell. A lesser force would be required to indent the gum as the cusps of the occlusion surface would more easily penetrate the gum shell. Six pieces of gum were tested and the maximum value required to break the gum shell recorded.

To be able to measure occlusion force in the future, a direct

intraoral sensing device was designed. A custom-built dental arch shape bite sensor was designed and prototyped with a bite registration feature using an off-the-shelf force transducer. The prototype with protective layers held three FlexiForce A301 sensors on the correct anatomical positions of teeth. These positions were incisor and two posterior working and non-working side on 2nd molars. The design of dental arch was based on the digital skull as presented in Table 1 to make sure the sensitive area of the sensor pads sat correctly on the occlusal surfaces of the teeth.

The purpose of fabricating such custom-built bite sensors (Tekscan, Inc., South Boston, Massachusetts, FlexiForce A301) was for future comprehensive study for comparison among the robot, human, commercial compression, and torsion testing machines and Apparatus A & B to investigate the mechanics of chewing sequences, shearing, crushing and grinding for effective release of xylitol, nicotine, caffeine occurred during the first 5 minutes of chewing a MCG.

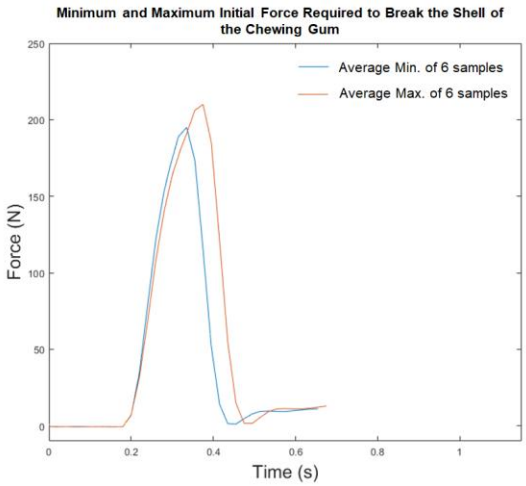

Fig. 3 Initial force required to break the shell of the chewing gum using an Instron 50KN Static Load Cell

Table II highlights the different features of the chewing simulator.

TABLE II

The descriptions and specifications of the chewing simulator

Functionalities	Specifications
The release of xylitol from chewing gum • Upper jaw, fixed • Lower jaw, mobile	• Initial sample: 1- 5 g • Cycle time from 1 s • Chewing up to 1200 s • Forces up to 300 N • Chewing frequency 1 s at a constant speed, 60 chews per minute • Maximum volume supply as necessary • Working volume up to 47 mL
Crushing, shearing and grinding of chewing gum	The condyle brackets with built in chewing pattern and bilateral functional springs replicate the Bennet movement of the mandible
Closed chewing chamber • Teeth • Artificial cheeks	The removable closed chewing chamber contain a set of maxillary and mandibular replica teeth and artificial cheeks • Holes on the surface of the teeth allow air and artificial saliva to enter • Artificial cheeks encapsulate the chewing chamber preventing the gum from leaving the occlusal surface and the artificial saliva from leaking
Tongue	Pneumatic manipulation of the chewing gum in the closed chewing chamber simulates the action of the cheeks and tongue to re-shape and re-orient the chewing gum
Fluids	Artificial saliva inlet: up to 5 mL/min continuous flow
Controls • Temperature • Motion and forces • Volume	• Water used to maintain the chewing chamber at 37 ºC • The cam, 4-bar linkage and condyle brackets with built in chewing pattern and bilateral functional springs dictate the chewing trajectory emulating the Bennet movement of the mandible allowing various forces to be applied to the bolus in accordance to its stiffness • Saliva flow determined by micro pump circulation
Sampling	A Universal tube is attached external to the chewing chamber via a connecting tube to collect the artificial saliva containing the released agents from the gum.
Practical aspects	• Removable closed chewing chamber • Easy dismantling, cleaning and sterilising if necessary • Ease of sampling • No lubricant

B. Saliva Flow Rate and Volume Calculations during Chewing

The custom built-in control box had to be programmed to simulate the increasing and decreasing production of artificial saliva delivered into the chewing chamber over the 20 minute chewing period. Clinical data [92] were used and processed with MATLAB ver. R2018b to evaluate the flow rate of saliva produced in the human mouth over 20 minute period while chewing. Fig. 4 shows that the saliva flow rate reaches a peak value of 4.8 ml/min at the beginning of a chewing period. Then, the flow decreases tending towards a value of around 1.2 ml/min. The data points were then linearly interpolated to give the approximate values of saliva flow rate every 30 seconds and plotted to produce a saliva flow rate versus time curve. Numerical integration was then used to approximate the quantity of saliva produced in each 30 second period as shown in Fig. 5.

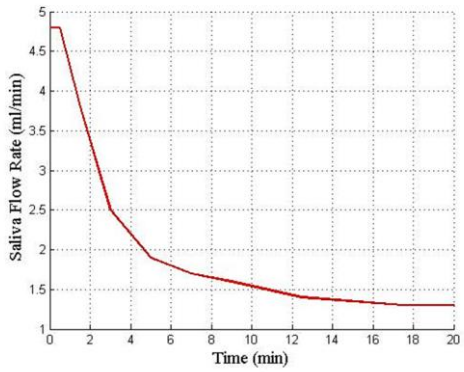

Fig. 4 Evaluation of saliva production in a human mouth over a 20 minute period while chewing

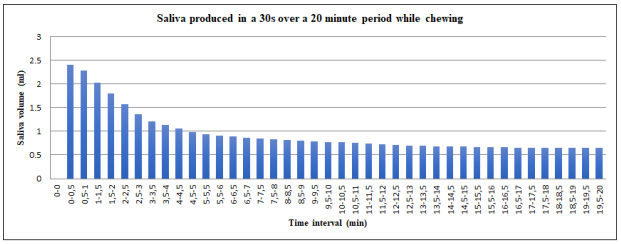

Fig. 5 Evaluation of the artificial saliva volume delivered in the chewing chamber per minute over a 20 minute period while the robot chew

C. Determining Xylitol Release Using Human Participants and the Chewing Simulator

Ten participants completed this study (8 females and 2 males) and there were no reported adverse events.

The mean amount of saliva collected over the 20 minute period from the human participants was 25.17 ml. The mean amount of artificial saliva solution recovered from the chewing simulator when 23.5 ml artificial saliva was delivered into the chewing chamber was 5.35 ml. The mean amount of solution recovered after 47 ml of artificial saliva was delivered into the chewing chamber was 21.12 ml.

The chewing chamber, with its chewing mechanism, was able to continually chew the gum into a bolus over a 20 minute period. The gum bolus recovered from the chewing chamber imitated that of the gum bolus following 20 minutes of chewing by human participants.

The mean amounts of xylitol released into the saliva solutions following each 5 minute time period using both human and robot chewing method are presented in Fig. 6. The amount of xylitol recovered from the bolus and from an unused piece of gum is also presented.

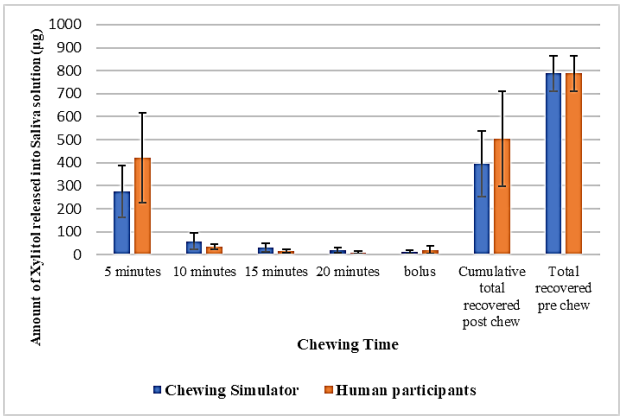

Fig. 6 Amount of xylitol released from chewing gum into saliva and artificial saliva using human participants and a chewing robot (n = 10). Error bars show standard deviations.

The results show that irrespective of the chewing mechanism, the greatest amount of xylitol was released from the chewing gum within the first five minutes of chewing. The amount of xylitol that was released for the later time periods decreased with each collection time. The overall trend for xylitol release was similar over the 20 minute chewing period irrespective of the chewing mechanism. The cumulative total amount of xylitol recovered from each time period and the amount recovered in the gum bolus were also similar irrespective of the chewing mechanism ($p = 0.08$), 20.55(µg) for human participants and 12.33(µg) for the chewing robot. Statistical analysis (Mann Whitney) comparing the amount of xylitol that was collected in the saliva after chewing the test gum using both chewing mechanisms at each time period is shown in Table III.

TABLE III

Amount of xylitol recovered following chewing with the test gum in the robot and with human participants with the statistical comparison between both chewing methods at each measuring point (n = 10).

	Amount of xylitol recovered following chewing by human participants (µg)	Amount of xylitol recovered following chewing by the chewing robot (µg)	Mann Whitney Statistical comparison (P values)
5 minutes	422.74	275.46	0.049
10 minutes	35.63	58.09	0.151
15 minutes	16.23	32.67	0.041
20 minutes	9.68	19.00	0.096
Bolus	20.55	12.33	0.326
Cumulative values	504.83	395.09	0.082

The amount of xylitol in saliva that was collected following the first 5 minutes of chewing was greater following chewing by human participants than by the chewing simulator, but the difference only just reached significance at $p = 0.049$. There was also a significant difference between the amounts of xylitol

that were released after 15 minutes where the amount recovered using human participants was statistically less than the amount recovered using the chewing simulator ($p = 0.041$) but these values were relatively low compared to the total amount of available xylitol in the gum. There were no other significant differences between the amounts recovered at each other time point.

The total amount of recovered xylitol compared to the amount of available xylitol in unchewed gum was 64% following chewing using human participants and 50% following chewing using the chewing simulator. The amount of artificial saliva collected compared to the amount that was delivered into the chewing chamber was 38%.

There was no xylitol quantified within the solution collected from either human participants or the chewing robot following chewing with the Hubba Bubba negative control gum. This confirmed that there was no xylitol carry-over within the apparatus or the measuring procedure.

IV. Discussion

This investigation tested a novel closed system chewing robot, demonstrating minimal xylitol retained in the bolus after 20 minutes chewing, the recommended length of time for chewing gum after eating [93]. The xylitol release from chewing xylitol impregnated gum was similar to that achieved with human participant chewing, over a 20 minute period. Further, the trend of xylitol release, with time, was similar for both chewing methods. This novel robot is the first, to the authors' knowledge, chewing simulator with built-in humanoid jaws and its removable chamber that attempts to accurately replicate human mastication and that closely mimics the human physiological features and mechanics of mastication, one of the greatest challenges faced in developing MCG [94].

Previous *in vitro* work investigating the release of substances from medicated chewing gums has involved techniques varying from the two instruments, recognised by the European Pharmacopoeia, known as apparatus A and B [19], [24]-[25], [95], to the use of a pestle and mortar to pound the chewing gum in solution releasing the agent of interest [96]. When analysing these methods it was clear that the human physiological features with mechanics of mastication and six degrees of freedom that are possible with human mastication were not accounted for limiting their applicability to modeling MCG drug release from chewing. This work presents a chewing simulator that replicates these whilst more closely reproducing the Bennet movement of the mandible, curve of Spee, curve of Wilson and sphere of Monson. This manuscript describes the chewing robot with built-in humanoid jaws design process and provides proof of principle that a simulator of this type can closely replicate human mastication and the amounts of agents released from chewing gum. At this initial stage, a direct comparison with Apparatus A and B was not undertaken, but will be investigated in future studies. A similar version of the chewing simulator, where the six degrees of freedom is taken into account to more closely simulate human mastication, has previously been designed by our group and successfully used to test dental materials in an open system [15], [97]. This newly developed robotic system operates with a closed chamber allowing the flow of solution through the system where it can then be collected and measured. The closed chamber also enables the chewing gum to remain on the occlusal surfaces of the teeth during mastication. This design allows commercially available gum to be sheared, crushed and ground in a comparable fashion to human mastication, applying forces up to 250 N to initially break through the hard shell of the chewing gum. The design of the spring functionality also allowed a varied amount of force to be applied during chewing based on the stiffness of the gum bolus. The resulting final robotic gum bolus reflected the human chewed gum bolus, after 20 minutes chewing of each, with both retaining minimal xylitol quantities. This demonstrates that the chewing mechanism of the simulator with built-in humanoid jaws has potential to replicate human mastication and that further work is required to validate the system.

The delivery of a solution is a necessity when simulating the chewing of gum, as it enables the release of agents within the gum. The amount of solution that is used in an *in vitro* simulator also determines the dilution of the agent released. It is important to deliver the volume of solution representative of the amount that would be expressed into the oral cavity during the mastication cycle. The volume of saliva flow within the oral cavity varies between individuals as well as within a chewing cycle [98]. The amount of solution delivered over the 20 minute chewing cycle used in this study was determined by previous work carried out by Cecilia Dong *et al.* [92] alongside some predictive calculations to identify how much solution may be lost due to evaporation from the pneumatic mechanism being used to tumble the chewing gum within the chewing chamber. The flow rate based on human clinical data [92] indicates that it reaches a peak value of 4.8 ml/min at the beginning of a chewing period. Then, the flow decreases tending towards a value of around 1.2 ml/min. Based on this information our calculations showed a total volume of almost 38 ml was produced in the mouth over the 20 minute chewing period. However, these values would only be valid for a complete human mouth. The chewing chamber of the simulator isolates three molars on one side of the mouth, so it is reasonable to accept that only half of the saliva produced interacts with this chewing area. There are three main salivary gland groups which are paired and mirrored in the sagittal plane [98] therefore the total quantity of artificial saliva delivered to the chewing chamber during a 20 minutes test was calculated to be about 19 ml, which is consistent with the 20 ml volume of artificial saliva recommended in a test cell by the European Pharmacopeia [24], [25]. However, in testing with 19 ml the final amount of solution recovered was lower than expected. The loss was potentially due/attributed to the evaporation of saliva from the system, and its adherence to the structures in the system. The amount of solution lost over the 20 minute chewing cycle was compensated for by increasing the quantity of solution delivered to the chewing chamber by the amount that it was calculated would be lost by evaporation. The fluid model computation analysis showed that 4.52 ml of artificial saliva could evaporate during 20 minutes of chewing, therefore the

total amount of artificial saliva required was 23.52 (19 +4.52)ml for the 20 minute operational period. This amount of solution was used for three chewing cycles, however there was concern that there would not be adequate recovered solution for analysis, thus the volume was doubled for the remaining samples with the calculations adjusted accordingly. However, when all the data had been analysed it was confirmed that the doubling of volume had not been necessary as the original 23.52 ml yielded sufficient for analysis.

The total volume of artificial saliva recovered from the chewing simulator was less than the amount that was delivered into the chamber. It is unavoidable that some saliva would be lost because it will be retained on the surfaces of the teeth and artificial cheeks, incorporated into the gum bolus and as previously mentioned, some will be lost due to evaporation through the pneumatic mechanism used in the chewing chamber. The action of changing the collection vessel every 5 minutes did not cause a loss of solution, taking only a couple of seconds, so any solution that may have been lost due to changing the collection pots was minimal.

The ideal solution to be added to a chewing simulator would be whole stimulated human saliva to most closely represent the oral cavity, but human saliva is not a stable solution once in the environment and degrades rapidly. It is also difficult to replicate the actual composition of human saliva in the laboratory but there are various artificial salivas that are widely accepted for *in vitro* investigations [99]. Even though the European pharmacopoeia suggests using phosphate buffered saline when using the chewing simulators known as Apparatus A and B, it was decided that for this study we would use an artificial saliva that more closely represents the minerals within human saliva. The artificial saliva that was used in this study was a modified version of the one that was developed by Peter Shellis [100]. It has been used in previous studies [101]-[102] and represents a solution that is moderately supersaturated with respect to hydroxyapatite, slightly supersaturated with respect to octacalcium phosphate and approximately saturated with respect to dicalcium phosphate dihydrate Further work in developing the chewing simulator is required to determine the most appropriate artificial saliva to investigate the release of agents from MCG. It will be interesting to determine how the inclusion of mucins, enzymes and organic compounds, which are often included in artificial saliva, may affect the rate of release from chewing gums.

The amount of xylitol that was recovered from the artificial saliva following each 5 minute time interval was similar to the amount that was recovered when using human participants, showing the potential of the chewing robot. The variance in xylitol released over the ten cycles being explained in terms of random movement of the gum during the robotic chewing cycle, similar to the random nature of human chewing, which also showed variance, demonstrated in Figure 6. Interestingly 36% of the xylitol was not recovered in the human participants. Although a great number of studies about the properties of xylitol have been conducted, its exact mechanism of action has not yet been understood [103]. It is known that xylitol forms complexes with ions displacing the water molecules, which could contribute to concentrating xylitol in an environment such as the human buccal mucosa following its consumption [104]. These characteristics may contribute to loss of xylitol due to its adherence to, or absorption through, the buccal mucosa. As all the volunteers had been trained to expectorate their saliva into collecting vessels, swallowing the saliva was not an explanation of loss. Fifty percent of the xylitol was lost in the chewing robot, most likely due to loss of saliva in the mechanism of the robot as described or adherence of xylitol to the surface materials of the chewing robot. The authors acknowledge that the materials of the chamber could have been washed to capture some of this loss and the robot needs adaptation to minimise evaporation in the closed system.

Irrespective of artificial saliva that was lost during the chewing cycle, it was encouraging to see that the amount of xylitol that was left in the gum bolus after 20 minutes chewing by both methods was very low at 2.6% following chewing by human participants and 1.6% following chewing by the chewing simulator. This shows that nearly all of the xylitol had been released into solution, confirming that the chewing simulator was effective in releasing the agent from the chewing gum at a similar rate to human participants. A combination of the similarities between the mastication action of the simulator and the human jaw along with the air supply, pumps and pneumatic solenoid valve that are built into the control box to enable tumbling of the gum in the chewing chamber, meant that exposure of all of the gum surface to the saliva was possible which enhanced the dissolution delivery of xylitol. Previous work by Catharina Kvist *et al.* [19] and [26] has also shown that when using Apparatus B as a chewing simulator, the amount of xylitol that was released from the chewing gum was mostly released within the first 20 minutes of chewing, which correlates well with the amount released from the chewing robot. This work is the first stage in validating the system. This work has shown potential to reproduce human mastication and further work is required.

V. CONCLUSION

A chewing robot with built-in humanoid jaws to closely replicate the human masticatory action was successfully developed. The robot demonstrated similar *in vitro* release of xylitol, from a commercially available chewing gum, to that which was recorded *in vivo*, compared through the amount of xylitol recorded in both of the boluses post chewing although it is recognised that the sample size was small. The vast majority of the xylitol was released after 20 minutes irrespective of chewing methods, with the greatest amount released during the first 5 minutes.

Future developments of the chewing simulator, such as creating different chewing patterns, will increase the robot's versatility. The manually driven robot could be automated to make sampling and investigation more efficient in the future. The development of a chewing robot that closely replicates human mastication provides opportunities for pharmaceutical companies to investigate and refine drug release from gum, with reproducible results, reduced patient exposure and reduced

costs using this novel methodology. There are many advantages to developing MCG but in order to develop them safely and cost effectively it is beneficial that reproducible *in vitro* investigations are first performed.

ACKNOWLEDGMENT

A favourable ethical approval was granted for this study by the University of Bristol Faculty of Health Sciences Research Ethics Committee. Application No. 30882.

REFERENCES

[1] Jacobsen *et al.,* (2004). Medicated Chewing Gum: Pros and Cons. *Am J Drug Deliv. 2 (2)*:75-88.
[2] Imfeld T. (1999). Chewing gum-facts and fiction: a review of gum-chewing and oral health. *Crit Rev Oral Biol Med. 10(3):*405-19.
[3] Buzalaf *et al.,* (2018, Mar 9). Prevention of erosive tooth wear: targeting nutritional and patient-related risks factors. *Br Dent J. 224(5)*:371-378. doi: 10.1038/sj.bdj.2018.173.
[4] Newton *et al.,* (2019, Nov 9). A Systematic Review and Meta-Analysis of the Role of Sugar-Free Chewing Gum in Dental Caries. *JDR Clin Trans Res.* :2380084419887178. doi: 10.1177/2380084419887178.
[5] T. Al Hagbani and S. Nazzal. (2018). Medicated chewing gums (MCGs): composition, production and mechanical testing. *AAPS Pharm. Sci. Tech. 19*, pp. 2908–2920.
[6] Hansson *et al.,* (2019, Nov 21). Effect of nicotine 6 mg gum on urges to smoke, a randomized clinical trial. *BMC Pharmacol Toxicol. 20(1)*:69
[7] T. Al Hagbani and S. Nazzal. (2017). Curcumin complexation with cyclodextrins by the autoclave process: method development and characterization of complex formation. *Int. J. Pharm. 520*, pp.173–180.
[8] T. Al Hagbani and S. Nazzal. (2018). Development of postcompressional textural tests to evaluate the mechanical properties of medicated chewing gum tablets with high drug loadings. *J. Text. Stud. 49*, pp.30–37.
[9] T. Al Hagbani *et al.,* (2018). Mechanical Characterization and Dissolution of Chewing Gum Tablets (CGTs) Containing Co-compressed Health in Gum® and Curcumin/Cyclodextrin Inclusion Complex. *AAPS PharmSciTech*, pp1–9.
[10] M.R. Rassing. (1994). Chewing gum as a drug delivery system. *Adv. Drug Del. Rev. 13*, pp.89-121.
[11] P. Morell *et al.,* (2014). Understanding the relevance of in-mouth food processing. A review of in vitro techniques. *Trends Food Sci. Tech. 35*, pp.18-31.
[12] M.A. Peyron and A. Woda. (2016). An update about artificial mastication. *Food Sci. 9*, pp.21-28.
[13] C. Salles *et al.,* (2007). Development of a chewing simulator for food breakdown and the analysis of in vitro flavour compound release in a mouth environment. *J. Food Eng. 82*, pp.189-198.
[14] A. Woda *et al.,* (2010, Jun.). Development and validation of a mastication simulator, *Journal of Biomechanics, Volume 43, Issue 9*, pp.1667-1673.
[15] K. Alemzadeh, and D. Raabe. (2008). Prototyping artificial jaws for the robotic dental testing simulator. *Proc. Inst. Mech. Eng. H. 222*, pp.1209-1220.
[16] A. Grau *et al.,* (2018). Reliability of wear measurements of CAD-CAM restorative materials after artificial aging in a mastication simulator. *J. Mech. Behav. Biomed. Mater. 86*, pp.185-190.
[17] M. Steiner *et al.,* (2009). In vitro evaluation of a mechanical testing chewing simulator. *Dent. Mater. 25*, pp.494-9.
[18] L.L. Christrup and N. Møller. (1986). Chewing gum as a drug delivery system I: In vitro simulation of human mastication and influence of formulation upon release of a water soluble drug. *Arch. Pharm. Chem. Sci. Ed. 14*, pp.30-36.
[19] C. Kvist *et al.,* (1999). Apparatus for studying in vitro drug release from medicated chewing gums. *Int. J. Pharm. 189*, pp.57-65.
[20] M.A. Peyron *et al.,* (2018). Oral declines and mastication deficiencies cause alteration of food bolus properties. *Food Funct. 21*, pp.1112-1122.
[21] A. Tarrega *et al.,* (2019). Effect of Oral Physiology Parameters on In-Mouth Aroma Compound Release Using Lipoprotein Matrices: An In Vitro Approach. *Foods. 8*, E106.
[22] A. Grau *et al.,* (2018). Reliability of wear measurements of CAD-CAM restorative materials after artificial aging in a mastication simulator. *J. Mech. Behav. Biomed. Mater. 86*, pp.185-190.
[23] M. Steiner *et al.,* (2009). In vitro evaluation of a mechanical testing chewing simulator. *Dent. Mater. 25*, pp.494-9.
[24] European Pharmacopoeia. Dissolution test for medicated chewing gums monograph 2.9.25. In: European Pharmacopoeia, 9th ed.; European directorate for the quality of medicines, Council of Europe: Strasbourg, France. 340-344. 2016.
[25] L. Zieschang *et al.,* (2018). In vitro performance testing of medicated chewing gums. *Diss. Tech. 25*, pp.64–68.
[26] L.C. Kvist *et al.,* (2000). Equipment for drug release testing of medicated chewing gums. *J. Pharm. Biomed. Anal. 22*, pp.405-411.
[27] A. Externbrink *et al.,* (2019). An in vitro approach for evaluating the oral abuse deterrence of solid oral extended-release opioids with properties intended to deter abuse via chewing. *Int. J. Pharm. 561*, pp.305-313.
[28] J. Gajendran *et al.,* (2010, Aug.). Product performance test for medicated chewing gums. *Diss. Tech.* pp.15–18.
[29] J. Gajendran *et al.,* (2012). In vivo predictive release methods for medicated chewing gums. *Biopharm. Drug Dispos. 33*, pp.417-424.
[30] J. Gajendran, "Performance testing of medicated chewing gums with the goal of establishing in vitro in vivo correlation". PhD thesis. Universitatsbibliothek Mainz. 2016.
[31] C. Stomberg *et al.,* (2017). Development of a New Dissolution Test Method for Soft Chewable Dosage Forms. *AAPS Pharm. Sci. Tech.18*, pp.2446-2453.
[32] S. Benazzi *et al.,* (2014). Comparison of occlusal loading conditions in a lower second premolar using three-dimensional finite element analysis. *Clin Oral Investig 18*, pp.369–375. Available: http://dx.doi.org/10.1007/s00784-013-0973-8.
[33] T.R. Katona and G.J. Eckert. (2017). The mechanics of dental occlusion and disclusion, *Clinical Biomechanics 50*, pp.84–91.
[34] T.R. Katona. (2009, Jun.) An engineering analysis of dental occlusion principles, *AJO-DO*, 696.e1-e8,
[35] T.R. Katona. (2013). Engineering analyses of the link between occlusion and temporomandibular joint disorders, *J. Stomat. Occ. Med. 6*, pp.16–21, DOI 10.1007/s12548-012-0068-1.
[36] T.R. Katona *et al.,* (2014). An analytical approach to 3D orthodontic load systems, *Angle Orthodontist, Vol 84, No 5*, pp.830-838, DOI: 10.2319/092513-702.1.
[37] P. Bourdiola and L. Mioche. (2000). Correlations between functional and occlusal tooth-surface areas and food texture during natural chewing sequences in humans, *Archives of Oral Biology 45*, pp.691- 699.
[38] S.P. Ungar. (2015). Mammalian dental function and wear: A review. *Biosurf. Biotribol. 1*, pp.25–41.
[39] P.W. Lucas, "Dental functional morphology. How teeth work" – Cambridge, Cambridge University Press. 2004, 355 pp. ISBN 0–521–56236–8. 2004, https://doi.org/10.1017/CBO9780511735011
[40] J.W. Osborn. (1987). Relationship between the mandibular condyle and the occlusal plane during hominid evolution: some of its effects on jaw mechanics. *Am. J. Phys. Anthropol. 73*, pp.193-207.
[41] J.W. Osborn. (1993). Orientation of the masseter muscle and the curve of Spee in relation to crushing forces on the molar teeth of primates. *Am. J. Phys. Anthropol. 92*, pp.99-106.
[42] H. Fukoe *et al.,* (2012). Three-dimensional analyses of the mandible and the occlusal architecture of mandibular dentition. *J. Stomat. Occ. Med. 5*, pp.119–129.
[43] E. Fanucci *et al.,* (2008). Bennett movement of mandible: comparison between traditional methods and a 64-slices CTscanner. *Oral Implantol. 1*, pp.15-20.
[44] L.F. Andrews. (1972). The six keys to normal occlusion, *Am. J. Orthod. 62*, pp.296-309.
[45] S.E. Nam *et al.,* (2013). Making three-dimensional Monson's sphere using virtual dental models. *J. Dent. 41*, pp.336-344.
[46] F.G. Spee. (1980). The gliding path of the mandible along the skull. *J. Am. Dent. Assoc. 100*, pp. 670-675.
[47] S.D. Marshall *et al.,* (2008). Development of the curve of Spee. *Am. J. Orthod. Dentofacial. Orthop. 134*, pp. 344-352.
[48] C.D. Lynch and R.J. McConnell. (2002). Prosthodontic management of the curve of Spee: use of the Broadrick flag. *J. Prosthet. Dent. 87*, pp. 593-597.
[49] G.S. Monson (1982). Original communications: Applied mechanics to the theory of mandibular movements. *Dent. Cosmos. 74*, pp.1039-1053.
[50] J-Y. Yoon and M.R. Riley. (2009, Sep.). Grand challenges for biological engineering, *Journal of Biological Engineering, 3:16*, pp.1-4.

[51] College of Fellows. (2013, Jul.) American Institute for Medical and Biological Engineering, Medical and Biological Engineering in the Next 20 Years: The Promise and the Challenges, *IEEE Trans. Biomed. Eng.* vol. 60, 7.
[52] P. Brey and S. Nagel, Bioengineering. In H. ten Have (Ed.), Encyclopedia of Global Bioethics. Springer. 2015.
[53] S-H. Chan *et al.*, (2016). Integration of Bioelectronics and Bioinformatics: Future Direction of Bioengineering Research, *J. Med. Biol. Eng. 36*, pp.751–754.
[54] A.K. Goel, D.A. McAdams, R.B. Stone (Editors). Biologically Inspired Design Computational Methods and Tools, Springer-Verlag London, 2014.
[55] K. Fu et al., (2014). Bio-Inspired Design: An Overview Investigating Open Questions From the Broader Field of Design-by-Analogy, *Journal of Mechanical Design · Transactions of the ASME, Vol. 136* , pp.111102-1-18.
[56] L.H. Shu *et al.*, (2011). Biologically Inspired Design Biologically Inspired Design, *CIRP Annals - Manufacturing Technology*, pp 673-693.
[57] R. Tan *et al.*, (2019). Creative design inspired by biological knowledge: Technologies and methods, *Front. Mech. Eng. 14 (1)*, pp 1–14. https://doi.org/10.1007/s11465-018-0511-0.
[58] J.K.S. Nagel *et al.*, (2010, Oct.). Function-based, biologically inspired concept generation, *AIEDAM, Volume 24 Issue 4*, pp. 521-535.
[59] J.K.S. Nagel *et al.*, (2018). Establishing Analogy Categories for Bio-Inspired Design *Designs, 2(4), 47,* pp.1-18; https://doi.org/10.3390/designs2040047
[60] H.C. Lundeen and C.H. Gibbs. "Advances in occlusion, chapter 1 (Dental Practical Handbooks)", Mosby, St. Louis. 1982.
[61] J. Koolstra and T. Van Eijden (1995). Biomechanical Analysis of Jaw-Closing Movements. *J. Dent. Res. 74*, pp.1564-1570.
[62] K. Alemzadeh *et al.*, (2007). Prototyping a robotic dental testing simulator, *Proc. Inst. Mech. Eng. H. 221*, pp. 385-396.
[63] J.R. Clark *et al.*, (2001, Mar.). Functional Occlusion: I. A Review, *Journal of orthodontics*, Volume: 28 issue: 1, pp. 76-81.
[64] T. Várady and R. Martin: "Reverse Engineering", Chapter 26, Handbook of Computer Aided Geometric Design, Eds.: G. Farin, Advanced surface fitting techniques. CAGD, 19, 1, pp.19–42. 2002.
[65] T. Varady and M.A. Facello, "New Trends in Digital Shape Reconstruction", R. Martin, H. Bez, M. Sabin (Eds.): Mathematics of Surfaces, pp. 395–412, Springer-Verlag Berlin Heidelberg 2005.
[66] T. Varady. (2008). Automatic Procedures to Create CAD Models from Measured Data, *Computer-Aided Design & Applications, 5(5)*, pp.577-588.
[67] W. Sun *et al.*, (2005). Bio-CAD modeling and its applications in computer-aided tissue engineering, *Computer-Aided Design 37*, pp.1097–1114.
[68] S. Benazzi and S. Senck. (2011, Apr.). Comparing 3-Dimensional Virtual Methods for Reconstruction in Craniomaxillofacial Surgery, *J Oral Maxillofac Surg, 69(4),* pp. 1184-1194.
[69] S. Benazzi *et al.*, (2009). Geometric morphometric methods for bone reconstruction the mandibular condylar process of Pico Mirandola, *The Anatomical Record 292:* pp. 1088–1097.
[70] S. Benazzi *et al.*, (2009). Geometric morphometric methods for three-dimensional virtual reconstruction of a fragmented cranium: the case of Angelo Poliziano, *Int J Legal Med 123:* pp. 333–344.
[71] S. Benazzi *et al.*, (2011). Using occlusal wear information and finite element analysis to investigate stress distributions in human molars, *J. Anat. 219*, pp. 259–272.
[72] S. Benazzi *et al.*, (2011). Quantitative Assessment of Interproximal Wear Facet Outlines for the Association of Isolated Molars *AJPA 144, pp.*309–316.
[73] M. Singleton *et al.*, (2011). Allometric and Metameric Shape Variation in Pan Mandibular Molars: A Digital Morphometric Analysis, *The Anatomical Record 294*: pp.322–334.
[74] J. Libby *et al.*, (2017, May). Modelling human skull growth: a validated computational model, *J. R. Soc. Interface 14(130)*: pii: 20170202. http://dx.doi.org/10.1098/rsif.2017.0202.
[75] A.L. Smith *et al.*, (2015). Biomechanical implications of intraspecific shape variation in chimpanzee crania: moving toward an integration of geometric morphometrics and finite element analysis. *Anat Rec (Hoboken). 298(1):* pp. 122–144 doi:10.1002/ar.23074.
[76] F.L. Bookstein, "Morphometric tools for landmark data". Cambridge: Cambridge University Press. 1991.
[77] F.J. Rohlf and L.F. Marcus. (1993). A Revolution in Morphometrics, *TREE vol. 8, no. 4*, pp. 129-132.
[78] B.G. Richmond *et al.*, (2005). Finite Element Analysis in Functional Morphology, *The Anatomical Record Part A, 283A*: pp. 259–274.
[79] N.V. Cramon-Taubadel et al., (2007). The problem of assessing Landmark error in geometric morphometrics: theory, method, and modifications, *Am J Phys Anthropol.;134(1)*: pp.24-35.
[80] P. Mitteroecker and P. Gunz. (2009). Advances in Geometric Morphometrics, *Evol Biol 36:* pp. 235–247.
[81] J. Zhang *et al.*, (2017, Jul.). A novel 3D-printed head phantom with anatomically realistic geometry and continuously varying skull resistivity distribution for electrical impedance tomography. *Scientific Reports, 7*: 4608, pp.1-9. DOI:10.1038/s41598-017-05006-8.
[82] V. Majstorovic *et al.*, (2013). Reverse engineering of human bones by using method of anatomical features, *CIRP Annals - Manufacturing Technology 62*, pp.167–170, http://dx.doi.org/10.1016/j.cirp.2013.03.081
[83] W.B. Downs (1956, Oct.). Analysis of dentofacial profile. *The Angle Orthodontist*, 26(4). pp. 191-212.
[84] J.A. McNamara. (1984), A method of cephalometric evaluation, *AJO-DO*, Volume 86, Issue 6, pp.449–469.
[85] J. J. Lee *et al.*, (1997). Gender and racial variations in cephalometric analysis. *Otolaryngology–Head and Neck Surgery, 117(4)*: pp.326–329.
[86] R.T.H. Abdullah *et al.*, (2006). Steiner cephalometric analysis: predicted and actual treatment outcome compared, *Orthodontics and Craniofacial Research, Volume:9, Issue:2*, pp. 77-83.
[87] M.B. Atit *et al.*, (2013). Mean values of Steiner, Tweed, Ricketts and McNamara analysis in Maratha ethnic population: A cephalometric study, *APOS Trends in Orthodontics*, 3(5), pp.137-151.
[88] B. Sagl *et al.*, (2019, Sep.). A Dynamic Jaw Model With a Finite-Element Temporomandibular Joint, *Frontiers in Physiology, Volume 10, Article 1156*, pp.1-12.
[89] W.L. Xu *et al.*, (2008). Mechanism, design and motion control of a linkage chewing device for food evaluation. *Mech Mach Theory, 43 (3)*, pp.376-389.
[90] C. Sun *et al.*, (2014, Jan.). Dynamics and Compliance Control of a Linkage Robot for Food Chewing, *IEEE Trans. Ind. Electron. VOL. 61, NO. 1*, pp.377-386.
[91] W. Singhatanadgit *et al.*, (2016). Effect of bidirectional loading on contact and force characteristics under a newly developed masticatory simulator with a dual-direction loading system, *Dental Materials Journal, 35(6)*, pp.952–961.
[92] C. Dong *et al.*, (1995). The effects of chewing frequency and duration of gum chewing on salivary flow rate and sucrose concentration. *Archs. Oral Biol. 40*, no. 7, pp.585-588.
[93] P.A. Nayak *et al*, (2014). The effect of xylitol on dental caries and oral flora, *Clin Cosmet Investig Dent.* 6: 89–94.
[94] C.K. Brown *et al.*, (2011). FIP/AAPS Joint workshop report: dissolution/in vitro release testing of novel/special dosage forms, *AAPS Pharm. Sci. Tech. 12*, pp.782–794.
[95] R.B. Shete *et al.*, (2015). Formulation of eco-friendly medicated chewing gum to prevent motion sickness. *AAPS Pharm. Sci. Tech. 16*, pp.1041-1050.
[96] V.L. Mudumba *et al.*, (2014). Evaluation and comparison of changes in microhardness of primary and permanent enamel on exposure to acidic center-filled chewing gum: an in vitro study. *Int. J. Clin. Pediatr. Dent. 7*, pp.24-29.
[97] D. Raabe *et al.*, (2012). Improved single- and multi-contact life-time testing of dental restorative materials using key characteristics of the human masticatory system and a force/position-controlled robotic dental wear simulator. *Bioinspir. Biomim. 7*, pp.1–17.
[98] G.B. Proctor. (2016). The physiology of salivary secretion. *Periodontol. 2000. 70*, pp.11-25.
[99] J. Pytko-Polonczyk *et al.*, (2017). Artificial saliva and its use in biological experiments. *J. Physiol. Pharmacol. 68*, pp.807-813.
[100] R.P. Shellis. (1978). A synthetic saliva for cultural studies of dental plaque. *Arch. Oral. Biol. 23*, pp.485-489.
[101] M. Eisenburger *et al.*, (2001). Effect of time on the remineralisation of enamel by synthetic saliva after citric acid erosion. *Caries Res. 35*, pp.211-215.
[102] M. Eisenburger *et al.*, (2001). The use of ultrasonication to study remineralisation of eroded enamel. *Caries Res. 35*, pp.61-66.
[103] A.S. Ferreira *et al.*, (2015). By Passing Microbial Resistance: Xylitol Controls Microorganisms Growth by Means of Its Anti-Adherence Property. *Curr Pharm Biotechnol. 16(1):* 35-42.
[104] K.K. Mäkinen, (2000). Can the pentitol-hexitol theory explain the clinical observations made with xylitol? *Med. Hypotheses, 54*(4), 603-613.